DOI 10.1002/pmic.201500403 *Proteomics* 2016, *16*, 1376–1380

DATASET BRIEF

Comparing isogenic strains of Beijing genotype *Mycobacterium tuberculosis* after acquisition of Isoniazid resistance: A proteomics approach

Luisa María Nieto R, Carolina Mehaffy and Karen M. Dobos

Department of Microbiology, Immunology and Pathology, College of Veterinary Medicine and Biomedical Sciences, Colorado State University, Fort Collins, CO, USA

We determined differences in the protein abundance among two isogenic strains of *Mycobacterium tuberculosis* (*Mtb*) with different Isoniazid (INH) susceptibility profiles. The strains were isolated from a pulmonary tuberculosis patient before and after drug treatment. LC-MS/MS analysis identified 46 *Mtb* proteins with altered abundance after INH resistance acquisition. Protein abundance comparisons were done evaluating the different bacterial cellular fractions (membrane, cytosol, cell wall and secreted proteins). MS data have been deposited to the ProteomeXchange with identifier PXD002986.

Received: October 18, 2015
Revised: January 6, 2016
Accepted: February 24, 2016

Keywords:
Isogenic strains / Isoniazid / Microbiology / Resistance / Tuberculosis

In United States, the tuberculosis (TB) rate has been decreasing since 1992, having a reported rate of three cases per 100 000 population in 2014 [1]. However, this country began to experience a severe interruption in the supply of isoniazid (INH) in 2012 [2]. INH is one of the most effective drugs to treat TB and to prevent active TB in persons with latent TB infection [3,4]. The INH scarcity affected the US TB programs and created incomplete treatment regimens that may lead to higher INH resistance rates over time.

Despite the proven success of INH against *Mycobacterium tuberculosis* (*Mtb,* the causing agent of TB), the understanding of its mechanism of action and development of resistance has been a slow process. INH is a prodrug that needs the bacterial enzyme KatG *(catalase-peroxidase)* to become active. Activated INH inhibits mycolic acids biosynthesis, cell division, nucleic acid synthesis and electron transport, among other bacterial processes [5, 6]. INH resistance mechanisms include mutations in multiple genes, most often in the *katG* gene.

Simultaneous to INH resistance development, *Mtb* can undergo further variations including changes in protein levels which in turn may counteract the potential fitness loss due to the new phenotype. A previous proteomic analysis compared INH susceptible (INHs) and resistant (INHr) strains of *Mtb* and found five proteins overexpressed in the INHr strains. These proteins were not related to any of the known INH resistance mechanisms [7].

In the present study, we worked with clinical isogenic pairs of *Mtb*, to evaluate the variation in the protein levels after development of INH resistance. Clinical isogenic pairs are strains with the same genotype which can be obtained from the same patient before and after treatment. Although rare, isogenic pairs provide a unique setting to study drug resistance mechanisms and potential loss in fitness due to mutations conferring drug resistance without confounding effects due to intrinsic genotype differences.

We compared the global protein abundance levels of a clinical isogenic pair of *Mtb* and classified the proteome changes according with their functional category. Two isogenic strains of *Mtb* were isolated from a HIV positive patient, alcoholic, and intravenous drug user diagnosed in 1994 with pulmonary TB at University General Hospital of Gran Canaria Doctor Negrín, Las Palmas, Spain. The isolate obtained after drug treatment failure, was INHr to both concentrations tested (0.2

Correspondence: Associate Professor Karen M. Dobos, Colorado State University Department of Microbiology, Immunology, and Pathology, 1682 Campus Delivery, Fort Collins, CO 80523, USA
E-mail: Karen.dobos@colostate.edu
Fax: +1(970) 491-1815

Abbreviations: **CFP**, culture filtrate proteins; **CW**, cell wall; **CYT**, cytosol; **INH**, isoniazid; **MDR**, multidrug resistance; **MEM**, membrane; **Mtb**, *Mycobacterium tuberculosis*; **NSAF**, Normalized spectral abundance factor

and 1.0 μg/mL). Both strains belong to the Beijing genotype, tested by restriction fragment length polymorphism RFLP - IS6110 [8] and spoligotyping [9]. Drug susceptibility profiles were confirmed for both strains using the agar proportion method [10] by National Jewish Hospital, Denver, CO. After INHr, the strain developed MDR (multidrug-resistance) phenotype (resistance to i and rifampicin) and was successfully treated with second line drugs.

Bacteria culture condition, Culture Filtrate Protein (CFP) preparation, subcellular fractionation and proteomic analysis were performed as previously described with minor modifications [11]. Briefly, three biological replicates of each strain were cultured in one liter Glycerol-Alanine-salts media. The preparation of CFP and cell fractions required an initial filtration step (using a 0.2μm filter) and γ irradiation, respectively. Bacterial death was confirmed using the Alamar Blue assay (Invitrogen). CFP groups the secreted proteins and also those released onto the media during bacteria lysis. Cellular fractions include the mycobacterial membrane (MEM), cytosol (CYT) and cell wall (CW).

CFP was concentrated to a final volume of approximately 20 mL using a Millipore™ Amicon™ Bioseparations Stirred Cell with a 3-KDa mass cutoff membrane (Millipore). Concentrated CFP and CYT fraction were subjected to buffer exchange with 10 mM ammonium bicarbonate, using Amicon Ultra-15 centrifugal filter units with a 3-kDa molecular mass cutoff. The CW and MEM pellets were resuspended in 10 mM ammonium bicarbonate.

After the separation of CFP and mycobacterial cell fractions, protein was quantified by the bicinchoninic acid method (Thermo Scientific™ Pierce™). 30 μg of MEM, CYT and CFP were subjected to acetone precipitation, solubilization, reduction with dithiothreitol, alkylation with iodoacetamide, and trypsin digestion (using a mix of 1% ProteaseMaxTM Surfactant (Promega) and trypsin (Roche)) as described previously [11]. Following digestion, samples were desalted with Pierce® PepClean C18 columns (ThermoScientific) following the manufacturer instructions. CW proteins had a delipidation process [11] before to the protein digestion protocol described above.

One microgram of digested cellular fractions and CFP for all the three biological replicates were randomly analyzed in triplicate using LC-MS/MS as described previously [11]. Resulting raw data were converted into mzXML files using ProteoWizard [12]. LC-MS/MS spectra were then compared against *Mtb* genomic database (MtbReverse041712) using SORCERER (Sage-N Research, version 5.0.1). The parameters used for the analysis were: trypsin digestion, a maximum of two missed cleavages, a precursor mass range of 400 to 4500 amu, peptide mass tolerance of 1.5 amu, reduction and alkylation of cysteine residues (resulting in the addition of a carbamidomethyl group, 15.99 amu) and the oxidation of methionine (57.02 amu).

For each cellular fraction, peptide identifications from the MS/MS spectra previously searched were combined in the proteomic software Scaffold (version Scaffold 4.3.2, Proteome Software Inc., Portland, OR) summing all the technical replicates results for each biological sample. Normalized spectral abundance factor (NSAF) analysis was performed to measure the relative protein abundance [13]. Additional parameters required for the Scaffold algorithm for protein identification included a maximum of 5% of false discovery rate for peptide threshold as well as for protein threshold and at least of two peptides.

The MS proteomics data have been deposited to the ProteomeXchange Consortium [14] via the PRIDE partner repository with the dataset identifier PXD002986 and 10.6019/PXD002986. Differences between protein abundances among the two different susceptibility profiles were tested by two tailed Student's *t*-test.

We found 46 proteins either more or less abundant after acquisition of INHr (with $p < 0.05$) that were grouped in seven different categories (Fig. 1). These protein differences were mostly observed in the CFP (39.6%) and MEM (35.4%) fractions (Fig. 1, Table 1).

In our quantitative analysis, we particularly found low levels of KatG in the INHr isolate potentially explaining the resistance phenotype. The reduced levels of KatG were observed in all cellular fractions, except in the cell wall (Table 1). In addition to the role of activating INH, KatG is also involved in the *Mtb* response to reactive oxygen intermediates produced by phagocytes during intracellular infections [15], making this protein a well-studied virulence factor.

The category "Intermediary metabolism and respiration (IMR)" presented the highest number of proteins ($n = 20$) with variable abundance among the strains. In this category the enzymes from the tricarboxylic acid (TCA) cycle SucC, SucD (located in the same operon), Mdh, Acn and AceE were all decreased in the INHr strain (Fig. 2). AceE belongs to the aerobic oxidative TCA cycle. Additionally, two enzymes of the pentose phosphate pathway Gnd2 and Tal were also significantly different in this analysis but with higher and lower levels in the INHr strain, respectively (Table 1).

Among lipid metabolism, we detected differences in proteins involved in lipid biosynthesis and degradation pathways. For the former, FabG4 and Fas were increased in the INHr strain. FabG4 participates in the elongation of saturated fatty acids while Fas is a structurally integrated type I fatty acid synthase (FAS-I), similar to those found in eukaryotes. This particular enzyme has all catalytic domains contained within a single protein chain [16]. There were also enzymes identified in this study that belong to the FAS-II system, Rv0241 (HtdX) and Rv3389 (HtdY), but with different behavior. While HtdX had higher, HdtY had lower abundance levels in the INHr strain. Due to their sequence and structure, both enzymes are considered 3-hydroxyacil thioester dehydratases, but HtdX has a particular high capacity to produce lipoic acid and an increased preference for its substrate (3-hydroxyacyl-acyl carrier protein, ACP) [17]. In our study, HdtX trend was similar to the other enzymes involved in lipid biosynthesis. The different levels observed between HtdX and HtdY may

Table 1. Description of significantly different proteins in the INHr vs INHs Beijing strain comparison (*t*-test, $p < 0.05$)

Proteins significantly different (*t*-test, $p < 0.05$)	Gene name	Rv number	Functional category	Fold change (INHs/ INHr)[a)]
CFP (n = 19)				
Iron-regulated peptidyl-prolyl-cis-trans-isomerase A	ppiA	Rv0009	IMR	***1.6***
Chaperone protein DnaK	dnaK	Rv0350	V	0.5
Succinyl-CoA synthetase beta chain	sucC	Rv0951	IMR	***4.1***
Succinyl-CoA synthetase alpha chain	sucD	Rv0952	IMR	***3.9***
Enoyl-CoA hydratase EchA9	echA9	Rv1071c	L	***1.8***
6-phosphogluconate dehydrogenase, decarboxylating Gnd2	gnd2	Rv1122	IMR	***2.9***
Integration host factor MihF	mihF	Rv1388	IP	***1.7***
Transaldolase	tal	Rv1448c	IMR	0.5
Catalase-peroxidase-peroxynitritase T KatG	katG	Rv1908c	V	***14***
Conserved protein	Rv2204c	Rv2204c	C	0.5
Trigger factor protein	tig	Rv2462c	CW	***3.5***
Conserved protein	Rv2699c	Rv2699c	C	***3.9***
Adenosylhomocysteinase	sahH	Rv3248c	IMR	0.4
Thiosulfate sulfurtransferase	sseA	Rv3283	IMR	***3.6***
3-hydroxyacyl-thioester dehydratase HtdY	htdY	Rv3389c	L	***3.9***
10 kDa chaperonin (protein CPN10), MPT57	groES	Rv3418c	V	0.8
Conserved protein	Rv3433c	Rv3433c	C	0.2
Conserved membrane protein	Rv3587c	Rv3587c	CW	0.6
Secreted fibronectin-binding protein antigen protein	fbpD	Rv3803c	L	0.4
CW (n = 6)				
3-oxoacyl-[acyl-carrier protein] reductase FabG4	fabG4	Rv0242c	L	0.4
Acetyl-CoA acyltransferase FadA2	fadA2	Rv0243	L	0.5
Immunogenic protein MPT63	mpt63	Rv1926c	CW	***2.9***
ATP-dependent clp protease proteolytic subunit 2	clpP2	Rv2460c	IMR	0.5
Fatty-acid synthase (FAS)	fas	Rv2524c	L	0.3
Transcriptional regulator, crp/fnr-family	crp	Rv3676	R	0.1
CYT (n = 6)				
Two component system transcriptional regulator PrrA	prrA	Rv0903c	R	0.3
5-methyltetrahydropteroyltriglutamate-homocysteine methyltransferase MetE	metE	Rv1133c	IMR	***5.2***
Malate dehydrogenase	mdh	Rv1240	IMR	***1.3***
Phosphoglycerate kinase	pgk	Rv1437	IMR	***1.8***
Catalase-peroxidase-peroxynitritase T KatG	katG	Rv1908c	V	***61***
Aminomethyltransferase	gcvT	Rv2211c	IMR	0.2
MEM (n = 17)				
3-hydroxyacyl-thioester dehydratase HdtX	htdX	Rv0241c	L	0.09
Transport protein SecE2	secE2	Rv0379	CW	***1.3***
Polyprenyl-diphosphate synthase	grcC1	Rv0562	IMR	***INF***[b)]
50S ribosomal protein L23, RplW	rplW	Rv0703	IP	0.5
Phosphoribosylformylglycinamidine synthase II	purL	Rv0803	IMR	***1.7***
Transcription termination factor Rho	rho	Rv1297	IP	***1.9***
Thioredoxin	Rv1324	Rv1324	IMR	***3.2***
Iron-regulated aconitate hydratase	acn	Rv1475c	IMR	***1.3***
Glycine dehydrogenase	gcvB	Rv1832	IMR	***3.6***
Catalase-peroxidase-peroxynitritase T KatG	katG	Rv1908c	V	***2.6***
Monophosphatase	cysQ	Rv2131c	IMR	***7.5***
Pyruvate dehydrogenase E1 component	aceE	Rv2241	IMR	***1.2***
Conserved protein	Rv2402	Rv2402	C	***1.6***
Chorismate synthase	aroF	Rv2540c	IMR	0.4
Acyl-CoA dehydrogenase FadE22	fadE22	Rv3061c	L	0.5
Acyl-CoA dehydrogenase FadE32	fadE32	Rv3563	L	0.1
Enoyl-CoA hydratase EchA21	echA21	Rv3774	L	***2.7***

a) The quantitative method chosen for the statistical analysis and *p* value calculation was NSAF.
b) INF: NSAF in INHr strain was zero. IMR: Intermediary metabolism and respiration, V: Virulence, detoxification, adaptation, IP: Information pathways, L: Lipid metabolism, R: Regulatory protein, CW: Cell wall and cell wall processes, C: Conserved Hypothetical.

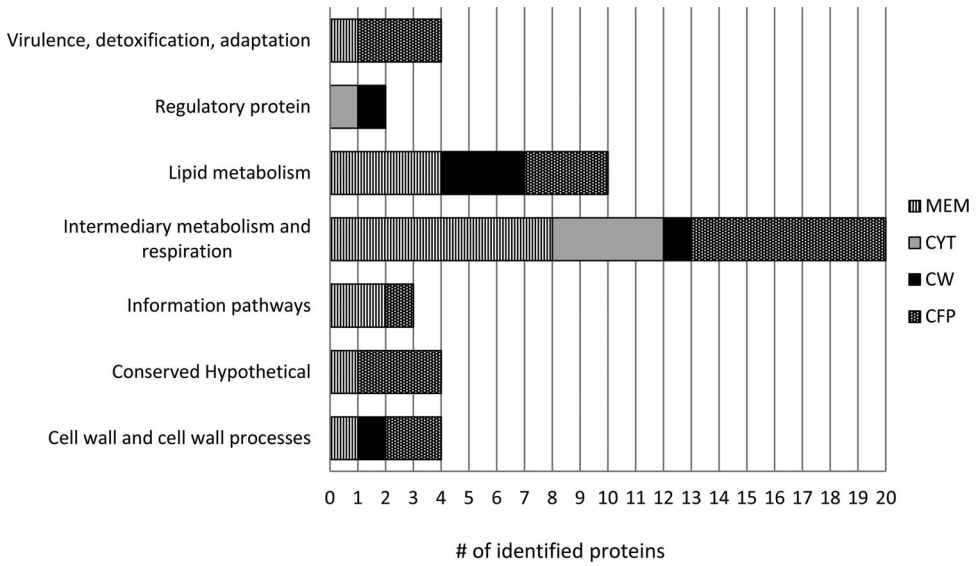

Figure 1. Functional categories of the *Mtb* proteins showing different levels among the INHs and INHr isogenic strains (p value <0.05). All categories are listed according to Tuberculist (version 2.6, Release 27 - March 2013, http://tuberculist.epfl.ch/).

be in line with results elsewhere indicating that HdtY may not be part of the ACP-dependent FAS-II system [17].

For fatty acid β oxidation, the dehydrogenases FadE22 and FadE32 and the acetyl-CoA acyltransferase FadA2 were increased while the crotonases EchA9 and EchA21 were decreased in the INHr strain (Table 1).

In summary, we demonstrated that acquisition of INH resistance can result in significant changes in the mycobacteria proteome, particularly in pathways related to respiration and lipid metabolism, both of which may result as a compensatory mechanism to the decrease in KatG abundance and its consequent impact on mycobacterial physiology and fitness.

This study was supported by the scholarship "Francisco Jose de Caldas-convocatoria 512" from the Colombian Administrative Department of Science, Technology, and Innovation Colciencias (recipient: Luisa Maria Nieto) and by the American Type Culture Collection fund #2010-0516-0005 (recipient: Karen Dobos). The authors thank Dr. Marcos Burgos, Medical Director of the Tuberculosis Program for the New Mexico Department of

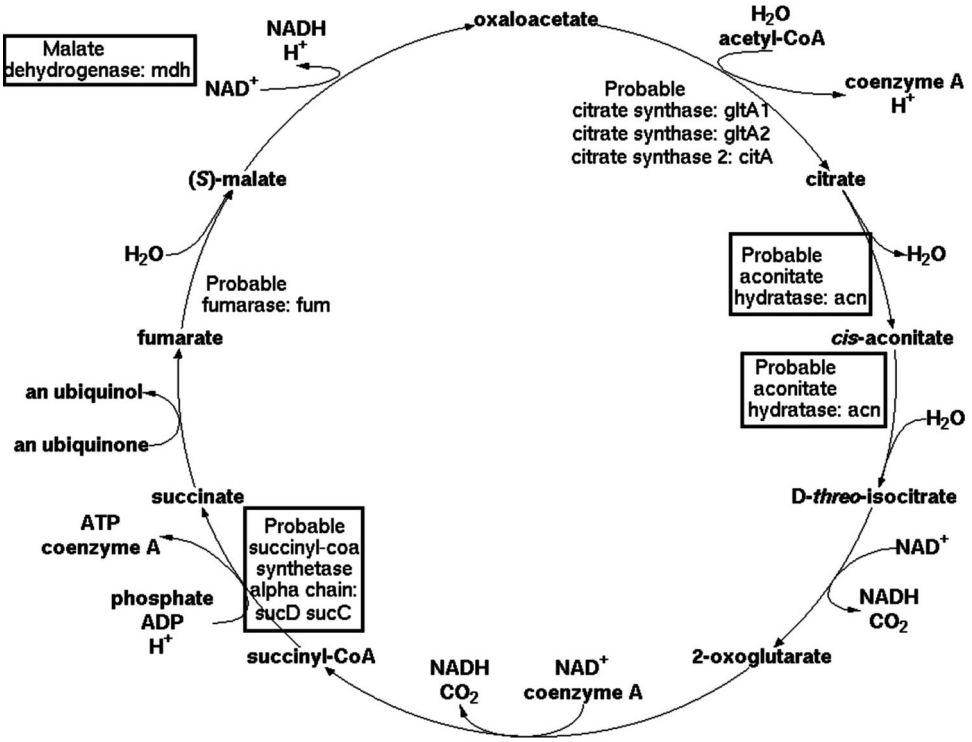

Figure 2. TCA cycle in *Mtb*. The enzymes in the boxes are reduced in the Beijing INHr strain. Adapted from http://biocyc.org/MTBRV.

Health, Jose A Caminero and Maria I. Campos-Herrero, Service of Pneumology and Service of Microbiology, University General Hospital, and Dr. Negrin, Las Palmas de Gran Canaria, Spain for provision of the clinical isolates from de-identified patient samples.

The proteomics MS data in this paper have been deposited in the ProteomeXchange Consortium (http://proteomecentral .proteomexchange.org) via the PRIDE partner repository [18]: dataset identifier PXD002986.

The authors have declared no conflict of interest.

References

[1] Scott, C., Kirking, H. L., Jeffries, C., Price, S. F. et al., Tuberculosis trends–United States, 2014. *MMWR Morb. Mortal. Wkly. Rep.* 2015, *64*, 265–269.

[2] (CDC), C. f. D. C. a. P., Impact of a shortage of first-line antituberculosis medication on tuberculosis control - United States, 2012–2013. *MMWR Morb. Mortal. Wkly. Rep.* 2013, *62*, 398–400.

[3] Zhang, Y., The magic bullets and tuberculosis drug targets. *Annu. Rev. Pharmacol. Toxicol.* 2005, *45*, 529–564.

[4] Getahun, H., Matteelli, A., Abubakar, I., Aziz, M. A. et al., Management of latent *Mycobacterium tuberculosis* infection: WHO guidelines for low tuberculosis burden countries. *Eur. Respir. J.* 2015, *46*, 1563–1576.

[5] Vilchèze, C., Morbidoni, H. R., Weisbrod, T. R., Iwamoto, H. et al., Inactivation of the inhA-encoded fatty acid synthase II (FASII) enoyl-acyl carrier protein reductase induces accumulation of the FASI end products and cell lysis of *Mycobacterium smegmatis*. *J. Bacteriol.* 2000, *182*, 4059–4067.

[6] Timmins, G. S., Deretic, V., Mechanisms of action of isoniazid. *Mol. Microbiol.* 2006, *62*, 1220–1227.

[7] Jiang, X., Zhang, W., Gao, F., Huang, Y. et al., Comparison of the proteome of isoniazid-resistant and -susceptible strains of *Mycobacterium tuberculosis*. *Microb. Drug Resist.* 2006, *12*, 231–238.

[8] van Soolingen, D., de Haas, P. E., Kremer, K., Restriction fragment length polymorphism typing of mycobacteria. *Methods Mol. Med.* 2001, *54*, 165–203.

[9] Kamerbeek, J., Schouls, L., Kolk, A., van Agterveld, M. et al., Simultaneous detection and strain differentiation of *Mycobacterium tuberculosis* for diagnosis and epidemiology. *J. Clin. Microbiol.* 1997, *35*, 907–914.

[10] B, K., G, K., *Public Health Mycobacteriology. A Guide for the Level III Laboratory*, Atlanta, GA 1985, Centers for Disease Control.

[11] Bisson, G. P., Mehaffy, C., Broeckling, C., Prenni, J. et al., Upregulation of the phthiocerol dimycocerosate biosynthetic pathway by rifampin-resistant, rpoB mutant *Mycobacterium tuberculosis*. *J. Bacteriol.* 2012, *194*, 6441–6452.

[12] Chambers, M. C., Maclean, B., Burke, R., Amodei, D. et al., A cross-platform toolkit for mass spectrometry and proteomics. *Nat. Biotechnol.* 2012, *30*, 918–920.

[13] Zhang, Y., Wen, Z., Washburn, M. P., Florens, L., Refinements to label free proteome quantitation: how to deal with peptides shared by multiple proteins. *Anal. Chem.* 2010, *82*, 2272–2281.

[14] Vizcaíno, J. A., Deutsch, E. W., Wang, R., Csordas, A. et al., ProteomeXchange provides globally coordinated proteomics data submission and dissemination. *Nat. Biotechnol.* 2014, *32*, 223–226.

[15] Ng, V. H., Cox, J. S., Sousa, A. O., MacMicking, J. D., McKinney, J. D., Role of KatG catalase-peroxidase in mycobacterial pathogenesis: countering the phagocyte oxidative burst. *Mol. Microbiol.* 2004, *52*, 1291–1302.

[16] Takayama, K., Wang, C., Besra, G. S., Pathway to synthesis and processing of mycolic acids in *Mycobacterium tuberculosis*. *Clin. Microbiol. Rev.* 2005, *18*, 81–101.

[17] Gurvitz, A., Hiltunen, J. K., Kastaniotis, A. J., Heterologous expression of mycobacterial proteins in *Saccharomyces cerevisiae* reveals two physiologically functional 3-hydroxyacyl-thioester dehydratases, HtdX and HtdY, in addition to HadABC and HtdZ. *J. Bacteriol.* 2009, *191*, 2683–2690.

[18] Vizcaino, J. A., Cote, R., Reisinger, F., Barsnes, H. et al., The proteomics identifications database: 2010 update. *Nucleic Acids Res.* 2010, *38*, D736–D742.

